International Journal of Basic and Applied Sciences, 14 (SI-2) (2025) 78-92

International Journal of Basic and Applied Sciences

Website: www.sciencepubco.com/index.php/IJBAS
https://doi.org/10.14419/7yk27p49
Research paper

Development of Comprehensive Design and Load Analysis of Free-Standing I- Beam Jib Cranes

Vijay Talodhikar [1, *], Pratik Girde [1], Manoj Kumbhalkar [2], Pramod Sahare [3], Tukaram S. Sargar [4], Nitin Kardekar [2], Sajid Shaikh [5], Shivakumar Khaple [6]

[1] Department of Mechanical Engineering, Tulsiramji Gaikwad Patil College of Engineering and Technology, Nagpur, India
[2] Department of Mechanical Engineering, JSPM Narhe Technical Campus, Pune, India
[3] Department of Mechanical Engineering, Rajiv Gandhi College of Engineering, Research and Technology, Chandrapur, India
[4] Department of Mechanical Engineering, Smt. Kashibai Navale College of Engineering, Pune, India
[5] Department of Electronics & Telecommunication Engineering, JSPM Narhe Technical Campus, Pune, India
[6] Department of Civil Engineering, JSPM Narhe Technical Campus, Pune, India
**Corresponding author E-mail:vijay.mechanical@tgpcet.com*

Received: March 26, 2025, Accepted: July 3, 2025, Published: July 18, 2025

Abstract

The hoist with trolley system is an integral part of A jib crane is a cantilevered instrument to typically secure to a column. The design and analysis of a unique floor-mounted I-beam jib crane is the main topic of this research. As the boom revolves, the trolley follows it, allowing for effective load management within a circle. The design process will account for the crane's weight and the loads it will lift to ensure stability and efficiency. This study aims to identify stress points in the crane's structure and propose reinforcement strategies to mitigate these induced stresses. A innovative comprehensive stress and load analysis will be conducted using analytical and software-based approaches. Reinforcing critical stress areas will enhance the crane's strength, durability, and operational safety. The goal is to develop a robust crane design capable of reliably handling specified loads, thereby improving efficiency and safety in industrial applications.

Keywords: *Design, structural analysis, I-Beam Jib Cranes, Modal analysis ,FEM (finite element method) technique.*

1. Introduction

Designed using three axial motions, a jib crane is a versatile lifting device it is rotate vertical, radial, and rotational. These three movements provide adaptability and precision, making the crane suitable for a different kind of tasks. The system consist a cantilevered monorail supported at one end, with a horizontal beam Used as a track for the hoist trolley. While versatile, jib cranes have more limitations, such as difficulty accessing tight corners, restricting their utility in specific task. Compact design of jib cranes ideal for smaller operational areas, particularly in specialized industrial applications requiring repetitive lifting and movement within a limited/operational radius [1].
Jib cranes have a range from a few meters to 50 meters and can lift weights from 0.5 to 200 tons. In order to handle large weights, these cranes are commonly utilized in port situations, building tasks, coastal areas, and various other outdoor settings. Standard jib cranes used for general cargo operations usually have a lifting capacity of
1.5 to 5 tons, and a 30-meter maximum height. specialized cranes with grabbing mechanisms can lift load up to 3 tons, operate at 50–100 cycles per hour, and achieve lifting heights exceeding 30 meters [2][3].
In shipyards and similar locations, jib cranes are often mounted on pontoons to lift large and heavy machinery. These heavy- duty cranes are engineered to manage loads ranging from 100 to 300 tons load carrying and are designed to ensure reliability under extreme operational conditions. Their robust construction enables them to withstand demanding environments while maintaining efficiency and durability [4].
Jib cranes play a most important role in industrial and construction environments, its provide solutions for lifting tasks. According to purpose one or two primary lifting winches are installed on these cranes, which can be operated either independently or in tandem, depending on the specific lifting requirements. In specialized settings, such as machine shops, auxiliary systems are often incorporated to handle lighter loads. These additional setups enhance operational flexibility and support intricate lifting operations, ensuring adaptability for diverse tasks [5]. Jib cranes installed on columns are very common in the packing sector. Designed to suit the operator's working height, these cranes efficiently handle loads of up to one ton. Their design ensures precision and safety, making them an ideal choice for a variety of packing operations. With a focus on meeting operational needs, these cranes are tailored to perform a range of tasks seamlessly, offering both reliability and effectiveness [4][5].
Overall, jib cranes are indispensable equipment in localized lifting applications due to their ability to lift load vertical, radial, and rotational movements. This versatility makes them suitable for an wide area or range of applications, from routine cargo handling to the lifting of heavy machinery. Their adaptability is further enhanced by customizable design features that address the unique demands of specific

environments. Whether deployed in industrial settings or on construction sites, jib cranes provide precise and efficient lifting solutions, ensuring safety and performance [6].
Through thoughtful design and operation, jib cranes continue to be a dependable choice for various lifting needs, combining durability, flexibility, and functionality. These qualities position them as an essential tool in addressing the challenges of localized lifting, ensuring optimal performance across different scenarios.

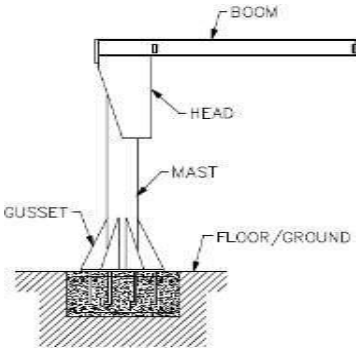

Fig 1: Free Standing Jib Cranes

2. Literature Review

A. Literature Survey

C. C. Dandavatimath et al. [1] studied on the bends in a jib crane's overhanging I section beam beneath self-weight plus load on the free end. New web form designs were created and tested using ANSYS FEM (finite element method) software to calculate how the geometric parameters affected the beam's bend or load carrying capacity. Further data from proposed designs were compared to standard beam . It has been discovered that improvements in web designs improve the load capacity or durability against twisting motion.
Fatimah De'nan, Musnira Mustar et al. [2] developed a model of finite elements in three dimensions using LUSAS 14.3 Software to look into how a beam of steel with a triangle-like web structure responds to shear bending force. A typical flat beam was used to compare beams of different thicknesses. The eigenvalue bending modeling was used to determine the buckling stress on a beam with a flat web as well as one with a triangle-like net form. According to the calculations, shear cracking was significantly impacted by different web thicknesses. Additionally, a web's corrugation thickness effectively improves the beam's shear bending capacity.
M. Dhanoosha et al. [5] involved the mathematical design and testing of A jib crane that makes utilization of FEM software. Models are produced in CREO with analytical design parameters and then examined in ANSYS. Two distinct kinds of steel were examined in order to assess the strain zones in a floor-mounted jib crane: ASME A36 steel and structural steel. The assessment revealed that ASME A36 steel demonstrated lower stress levels and reduced deformation compared to structural steel. This indicates that the ASME A36 alloy performs better in terms of minimizing structural strain and deformation under similar loading conditions, making it a more efficient option for reducing stress within the crane's structure.
R. K. Amreeta et al. [6] evaluates the stress generated by a single girder mounted on an external jib crane that can support 1000 kg of weight and span 2.5 meters, and a 180-level swing. Beam segments MB150, MB125, MB100, & a 140x80 rectangle section were studied analytically and numerically with ANSYS 14.5. The results demonstrated that MB150 is the best fit for the crane's specs. I-section beams have less stress and deformation than square parts, making them more robust. Furthermore, stresses in the supporting structure have been determined to be below allowed limits according to IS standards (IS 807:2006 & IS 15419:2004), proving the crane's safety.
S.M. Rajmane et al. [7] conducted an analysis of finite elements on the column-mounted jib crane. ANSYS software was utilized for modeling and analysis. During the course of the research, the impact of altering We investigated the effect of web depth and elevation on beam deflection with Von Mises stress. Deflection and stress produced by Von Mises can be observed diminishing as the web thickness increases. The deflection first reduces as web height rises, but then increases. Von Mises stress falls first, but subsequently grows and remains constant.
Amit S. Chaudhary et al. [8] studied I-section cantilever supports utilized in a jib crane bearing eccentric loads at self-weighted locations are examined for bend behavior, shearing capacity, and lateral torsional buckles. Multiple sections of cantilever beams, consisting of corrugated trapezoid or flat web parts, were studied using the FEA method in ANSYS. The study examines the impact of sectional characteristics such as web thickness, curvature angle, or infill length. The results reveal that trapezoid web sections give higher stiffness against lateral torsional buckling & bending than flat web sections. The bigger web width and increased net thickness further enhance stability and load resistance.
Ms Kavita R. Kapadni et al. [9] studied a conventional I section supported only by overhead crane beams carrying a significant load at its center in addition to its own weight, this study examines shear stresses, bending, and lateral torsion buckles. The study focused on lateral torsional buckling or bending, which are essential failure modes for beams. Warping and shear centering were also adjusted. To mitigate those problems, A design that features a changeable sectional shape with trapezoidal net was suggested as a substitute for a standard I-section beam.
S.S. Kiranalli et al. [10] used the FEM software ANSYS to investigate a jib crane. The crane was initially generated with a basic 2D element made up of a beam its a column, its the results were contrasted with analytical approaches to ensure that the mesh and parts were appropriate for three-dimensional analysis. In addition, a three-dimensional model was created and tested utilizing ANSYS to estimate the influence on changes in factors like web width or web elevation on the maximum potential displacement known as Von Mises pressure. It turns out that the amount of dissonance keeps decreasing as web height and breadth develop.
C. I. Gerdemeli et al. [21] investigated the shear bending on a steel beam with a triangular web form; a finite element model with three dimensions was constructed using LUSAS 14.3 Software. Beams of various thicknesses were compared with a standard flat beam. The buckles strain a beam with a straight web and one having a three-dimensional web shape was determined using eigenvalue bending analysis. The findings show that varying web widths have a significant impact on shear cracking. Furthermore, the web's curvature thickness helps to increase the beam's shear bending capacity.

Fatimah Denan et al. [24] done an empirical or numerical investigation to examine the compressive twisting action of segments of steel featuring trapezoid structures in a sideways direction. I-sections of 200 x 80 mm & 5 m in length have been examined for lateral torsional buckling. The critical buckling force was established using eigenvalue buckling analysis with finite element methods. The study found that steel beams having trapezoidal corrugated webs are more resilient than flat web beams to lateral torsional bending. Furthermore, thicker corrugation developed resistance because of a higher mechanical inertia around the minor axis.

B. Gap Identified

The reviewed studies have significantly contributed to the understanding of structural behavior in jib cranes, including the impact of geo-metric parameters on bending, shear capacity, and lateral torsional buckling. However, several gaps remain unexplored. Most studies focus on finite element modeling (FEM) using ANSYS software, yet there is limited research integrating experimental validation to complement numerical simulations [11-15]. The influence of advanced web designs, such as corrugated or trapezoidal sections, on both load-carrying capacity and overall stability has been explored, but further investigations are needed to optimize these designs for practical applications. Additionally, while various materials like ASME A36 steel have shown better performance in reducing stress and deformation, comparative studies involving modern high- strength materials are scarce. There is also a lack of studies addressing dynamic loading conditions, fatigue analysis, and real-world operational scenarios [16-20]. These gaps highlight the need for more holistic investigations that combine advanced modeling techniques with experimental and material studies to enhance jib crane design and performance

3. Research Methodology

A. Introduction to Beam and Jib Cranes:

Beams are important structural elements aimed at carrying loads parallel to their transverse axis. Their major function consists of transfer loads by bending and shear, making their load-bearing processes more complex than other structural components such as trusses or cables. While beams are primarily concerned with bending, additional phenomena like as shear, bearings, and buckling also occur. However, if the axial loads become sufficient, the component transforms into a "beam-column," indicating its dual role in axial and bending stresses.
Jib cranes, which are commonly employed in numerous industries in material handling, are normally made composed of both a vertical support (mast and pillar) with an overhead boom (jib) which carries a hoist mechanism. These cranes can rotate offer vertical, radial, and rotary movement, making them useful in a range of contexts including ports, building sites, and factories. Jib cranes have a wide load-carrying capacity, ranging from 0.5 tons to 200 tons, and can extend as much as fifty meters in length [22-23].
Finite element analysis is an example of advanced analysis methodologies (FEA), are essential for improving jib crane designs. FEA provides for a thorough study of the crane's stresses and performance under dynamic as well as static loads, which improves its safety, dependability, and overall effectiveness in operation.

B. Stability Analysis:

Stability analysis is critical for jib cranes to avoid accidents, particularly those caused by beam collapse. Common causes of breakdowns include lateral movements in the cantilever I- beam, twisting at the free end, and beam damage. Laterally torsional buckling (LTB) This occurs when an applied load induces lateral displacement or twisting, particularly in uncontrolled beams. Critical LTB load can be hard to calculate for slender I-girders, therefore lateral buckling is an important design consideration. Corrugated webs provide a solution by increasing stiffness and shearing buckling resistance, minimizing the requirement for stiffeners, enhancing fatigue life, and lowering fab-rication costs [25-27].

C. Methodology Adopted:

To solve a problem using FEM software, you must first define the answer domain, physical approach, boundaries, and physical attributes. Mesh generation is an additional phase that divides the model into smaller components for analysis. The steps in FEM analysis are critical to understanding complex systems.
The fundamental design of I-beam jib cranes is a sturdy boom connected to a pivot that can be fixed on a wall or a standalone column. The pivot enables 180° or 360° rotation, while the lifting mechanism, usually a pulley or motorised hoist, moves along the boom, providing a wide range of operations.

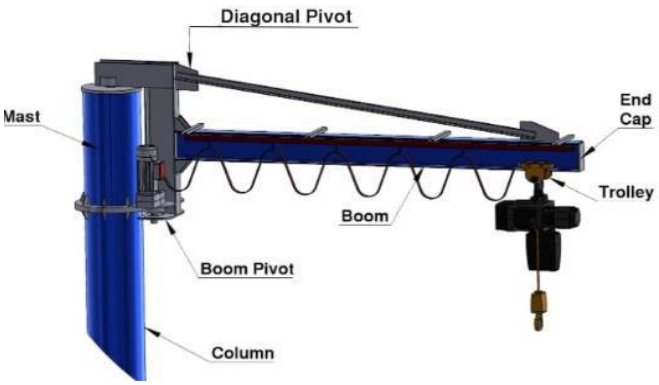

Fig 2: I beam jib crane installation

The I-beam Jib's loads the crane

1. Trolley mass: the sum of the weight of the entire trolley and each component.
2. The dead load is the sum of the weights of the bridge's operational parts, comprising any supporting equipment or stationary equipment.

3. Lifted force: The practical load consists of the weight on the raising apparatus.
4. Vertical forces of gravity are calculated as the dead loading proportion plus the hoist loading factor. According for the CMAA, the minimum load ration is 1.2, and the lifting load component is 0.15.
5. Drive inertia pressures: Such forces occur when shifting speeds and crane motions, and they are proportional to the torques utilized to drive and stop. Inertia forces and drives account for 2.5%, half the total number of vertical loads. Test loads should be 125 percent connected.

4. Methodology Adopted

Resolving any issue with FEM software is similar to resolving any other issue. Analytical definitions of our solution domain, physiological model, boundaries, and physical attributes are required. After that, resolve the issue and see what occurs. Mesh generation is an additional step that distinguishes numerical approaches from one another. In a situation that might been considered overly complicated, this step breaks the complex model up into smaller components [28-30]. The following procedures must be performed in order to use FEM software to address any problem:
Describe the qualities of the substance.
Define a collection of things that make up the item being modeled given that that component is available. This includes the properties of steel shown in Table 1.

Table 1: Properties of the Material

Properties	Value
Density	7850 kg/m^3
Poisson's Ratio	0.3
Young's modulus	2.1 × 10^5 MPa
Tensile Ultimate Strength	460 MPa
Tensile Yield Strength	250 MPa

Generate Mesh: To mesh the item, the mesh tool offers several possibilities. Depending on the user's needs, Both 2D or 3D meshes are possible. With careful selection, the specified areas or volume can be chosen and meshed.
Use loads: Adding constraints, such as boundaries and physical loadings, is the last stage once the system is fully built.
Obtain Solution: This is a stage since ANSYS has to identify the condition (steady state, transient, etc.) in which the problem needs to be fixed.
Obtain the Results: Following the solution's acquisition, ANSYS data can be presented in a variety of forms, including graphs, tables, or contour plots.

5. Work Plan

A. Selection of a Crane

The following crane characteristics are used in the selection of the Gorbel Crane FS-350 (put in Mounted) [31]:
- 500 kg of capacity;
- 360° rotation;
- 2.54 m boom span
- The minimum diameter is 300 mm

Dimensions of the Boom: Using the following section characteristics, As indicated in Table 2, I beams S10@25.4 lb/feet is selected from ASTM A6 [32].

Table 2: Beam Properties

Designation	Depth (mm)	Width of flange (mm)	Thickness of Web (mm)	Flange Thickness (mm)
S10×25.4	254	12.5	8	118

B. Load Calculations:

The following formula is used to determine the loads operating on the crane beam [5]:
1. Weight for the trolley: the total weight of the car plus any attached equipment.
2. The second dead loads is the beam or trolley's self-weight.
3. Hoist capacity: The sum of the weights of the hoisting apparatus and the operating load.
4. The dead load element plus the hoist load factor are the four forces that make up vertical inertia. The CMAA states that the hoist load element is 0.15 and the dead weight ratio is 1.2.
5. Forces of Inertia of Drive: These forces, which appear during speed fluctuations or crane motions, are reliant on the drive that produces the braking forces. 2.5 percent that the vertical load is equal to driving inertia forces.

Table 3 displays the results of the load calculation.The trolley is positioned at the free end of the beam for load calculations.

Table 3: Calculations of Crane Beam Load

1	Elevated Weight Because of the impact load factor Because of the dead load factor Tot	500 × 9.81 = 4905 N 0.25 × 4905 = 1226.25 N 0.5 × 4905 = 2452.5 N 8583.75 N = 8.58 kN
2	Dead Load causing trolley load	149.68 × 9.81 = 1.46 kN 1.2 × 1.46 = 1.752 kN
3	Lifted load + trolley load equals = vertical load	8.58 + 1.46 + 1.752 = 11.792 kN
4	2.5% of the vertical load is equal to the drive's inertia forces	2.5 × 11.792/100 = 11.792
5	Total Testing Weight	11.792 + 0.248 = 12.04 kN or 12040 N

C. Analysis of I Section Beams

First, the crane's conventional beam will be examined. For this, AutoCAD is used for modeling, and ANSYS is used for analysis; the process is described later in this chapter. To investigate and evaluate the buckling behavior of the beams, more beams with trapezoid corrugations within the web must be created. The suggested beam's top view is seen in Figure 3. 32 models having the following criteria are created and examined for this purpose.

Parameter selection:

The following parameters are chosen for the trapezoidal web:

i. Web width (tcw): 6 x 8 mm ii.30°, 45°, 60°, and 75° are the corrugation angles (θ)
ii. Length (b) of infill corrugation plate: 150, 250 mm
iii. Corrugation web width (h): 25, 35 mm.

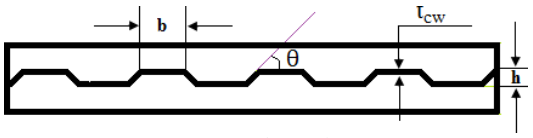

Fig 3: Web top view

The modeling

The models are made with AUTOCAD. As seen in Figure 3.(a), an AutoCAD model of a traditional I beam with an inclined web is first created. The specifications listed in Table 4 are used to construct an additional 32 models using trapezoid corrugated web.

Table 4: Corrugated web section parameters for different suggested beams.

Sr. No.	Web Thickness (mm)	Corrugation Plate Length (mm)	Corrugation Angles (Degree)	Corrugation width (mm)
Model 1	6	150	30^0	25
Model 2	8	150	30^0	25
Model 3	6	150	45^0	25
Model 4	8	150	45^0	25
Model 5	6	150	60^0	25
Model 6	8	150	60^0	25
Model 7	6	150	75^0	25
Model 8	8	150	75^0	25
Model 9	6	150	30^0	25
Model 10	8	150	30^0	25

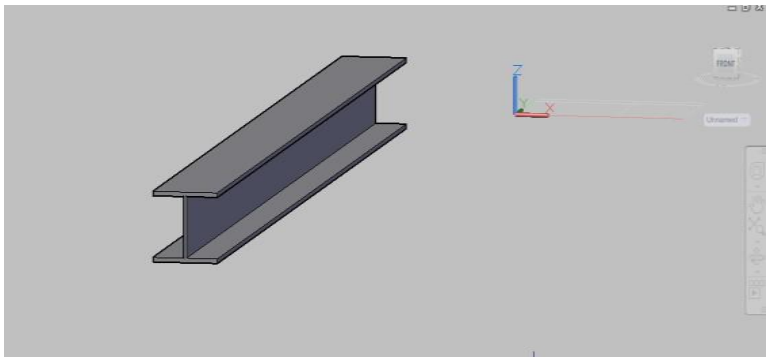

Fig 3. (a): Conventionally, a planar web is used, I beam.

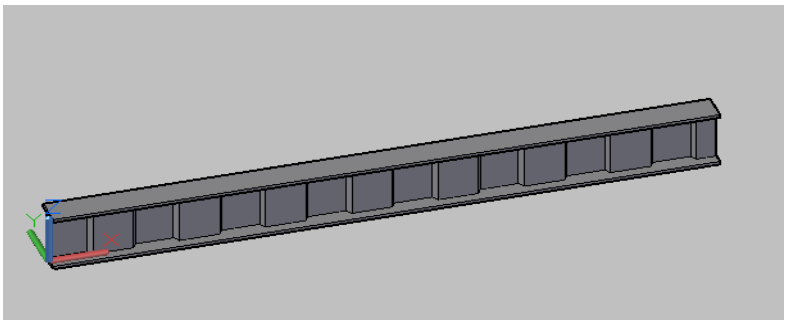

Fig 3. (b): I glow on the web with trapezoidal corrugations.

ANSYS analysis: ANSYS software is used for analysis. Below is an explanation of the analysis's process. The same process is used for both corrugated and flat beams:

Step 1: Data Engineering

As seen in Figure 4, the first phase of the study entails entering the technical data in the ANSYS program.

Developing the Geometry in Step Two

As seen in Figure 5, AutoCAD models are loaded into ANSYS to create geometry.

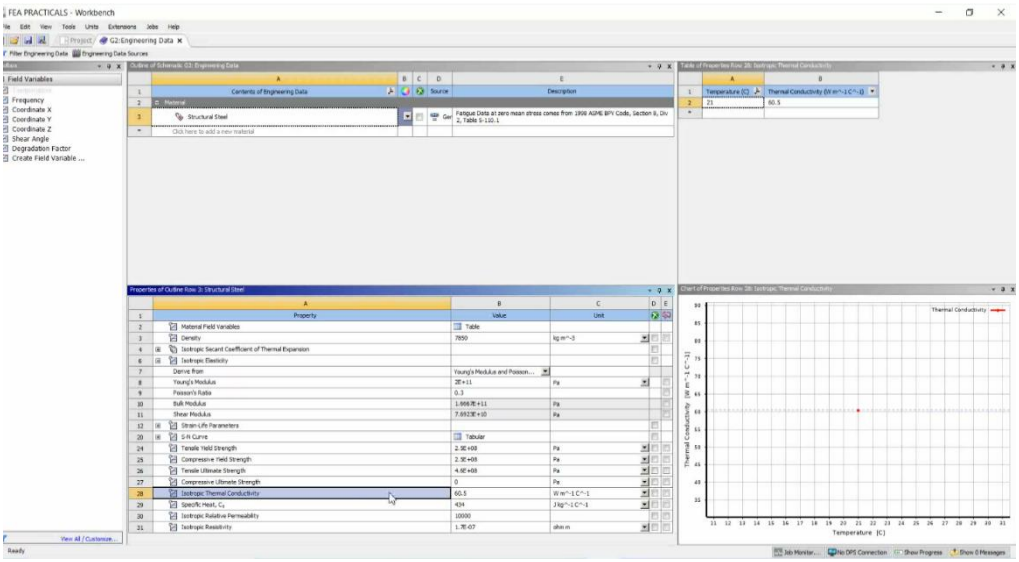

Fig. 4: ANSYS is supplied with engineering data.

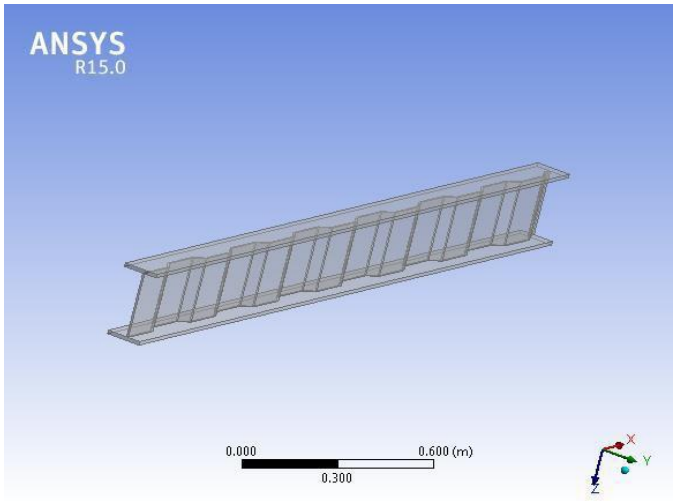

Fig. 5: ANSYS STEP 3: Import Geometry and Generate Mesh

To mesh the item, the mesh tool offers several possibilities. Depending on the user's needs, the mesh may be either 2D or 3D. Proper selection allows for the selection and meshing of certain areas or volumes. The size of the element was determined using a convergence analysis.

The data gathered following the convergence research is displayed in Table 5. Convergence occurs at a 10 mm aspect size, as seen in Figure 6. Thus, the analysis uses an element with a width of 10 mm.

Table 5: Convergence study data

Mesh Size (mm)	Number of Elements	Maximum Displacement (mm)
70	5598	7.5194
60	5793	7.5176
50	7406	7.4189
40	7763	7.5174
30	13509	7.5077
20	17015	7.4632
10	30536	7.6598
5	121776	7.6599

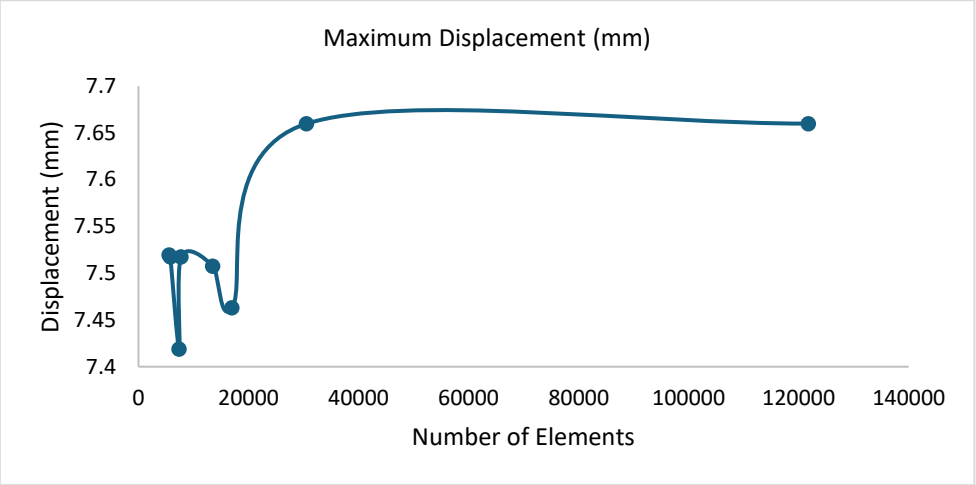

Fig. 6: Convergence analysis graph

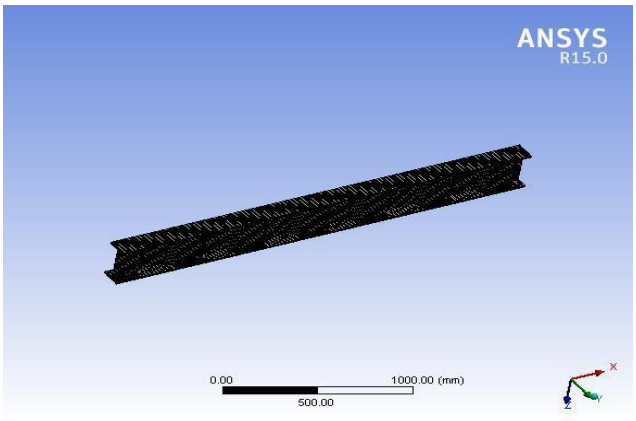

Fig. 7: Mesh Details

STEP 4: Conditions of Boundaries and Application of Load Adding constraints, such as boundary conditions or physical loadings, is the last stage once the system is fully built. A beam's left end is fixed for support, as shown in Figure 8, and all movement is restricted within its X, Y, and Z dimensions. In order to prevent stress concentration, the entire lifted weight of 12040 N is applied transversely, distributing it across a 118 x 100 mm space in the direction of the free end. Figure 9 illustrates how load is applied in ANSYS software.

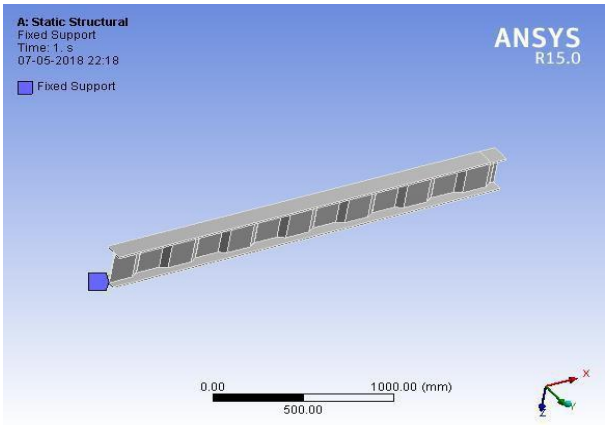

Fig. 8: The left end of the fixed support

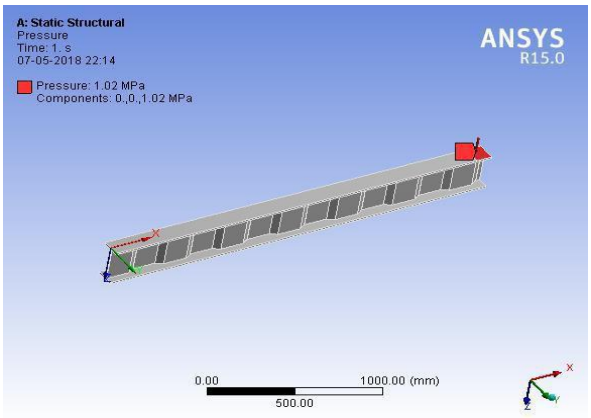

Fig. 9: Step 5: Load the Application and Get the Solution

Following the application of load, the models are examined for primary stress, Shear stress, buckling load, and von Mises stress.

6. Results and Discussion

6.1 FEA Results

6.1.1 Flat Beam FEA Results:

The buckling load, highest shear stress, and related stress data have been displayed in a table following a finite element analysis (FEA).4.1. The buckling load of just the initial mode is calculated by multiplying the applied load by the load converter.

Table 6: FEA findings for a beam level

Buckling Load (kN)	Maximum Shear Stress (MPa)	Equivalent Stress (MPa)	Maximum Principal Stress (MPa)
81.0	56.864	106.82	160.27

6.1.2 FEA Results for Corrugated Beam:

After finite element analysis, the bending load, highest shear stress, and associated stress data have been combined into a table.4.2 to 4.5 to see how the structural capacities are affected by the corrugation web's size.

Table 7: Corrugated beam FEA results for buckling load

Corrugation Plate Length	Web Width	Web Thickness	Buckling Load (kN)			
			30^0	45^0	60^0	75^0
150	25	6	71.32	84.73	86.48	87.84
		8	88.25	90.24	92.00	93.82
	35	6	85.44	87.71	94.48	94.76
		8	91.01	93.34	95.95	99.39
250	25	6	70.22	83.22	83.00	83.83
		8	86.57	88.81	89.80	89.85
	35	6	84.15	84.00	87.49	87.56
		8	89.28	90.05	93.45	93.731

Table 8: Corrugated beam FEA findings for maximum stress from shear

Corrugation Plate Length	Web Width	Web Thickness	Maximum Shear Stress (MPa)			
			30^0	45^0	60^0	75^0
150	25	6	64.36	61.32	60.27	60.00
		8	58.01	57.30	55.59	50.79
	35	6	61.31	60.93	55.34	53.00
		8	56.32	55.79	54.54	49.14
250	25	6	64.64	62.31	60.99	60.64
		8	58.07	57.33	56.143	55.82
	35	6	62.18	60.82	60.48	60.00
		8	57.28	56.64	55.71	54.11

Table 9: Corrugated beam FEA findings for equivalent stress

Corrugation Plate Length	Web Width	Web Thickness	Equivalent Stress (MPa)			
			30^0	45^0	60^0	75^0
150	25	6	118.5	113.39	111.10	110.93
		8	109.24	107.81	108.25	108.00
	35	6	108.42	107.57	106.61	105.99
		8	107.96	106.81	106.18	105.00
250	25	6	121.73	115.78	114.66	114.01
		8	109.99	109.34	109.27	108.72
	35	6	116.96	115.32	114.00	113.28
		8	110.32	109.08	108.35	107.23

Table 10: Corrugated beam FEA findings for Maximum Main Stress

Corrugation Plate Length	Web Width	Web Thickness	Maximum Principal Stress (MPa)			
			30^0	45^0	60^0	75^0
150	25	6	157.73	157.00	156.77	156.22
		8	156.55	156.43	155.07	155.01
	35	6	156.91	156.12	155.00	155.96
		8	156.42	156.00	154.20	154.82
250	25	6	158.06	157.93	157.91	156.99
		8	157.43	156.63	156.11	156.00
	35	6	157.96	157.45	156.65	156.28
		8	157.34	157.26	156.13	156.10

To further illustrate the impact of web waves on structure capabilities, the data have been displayed as graphs (Figure 10–11).

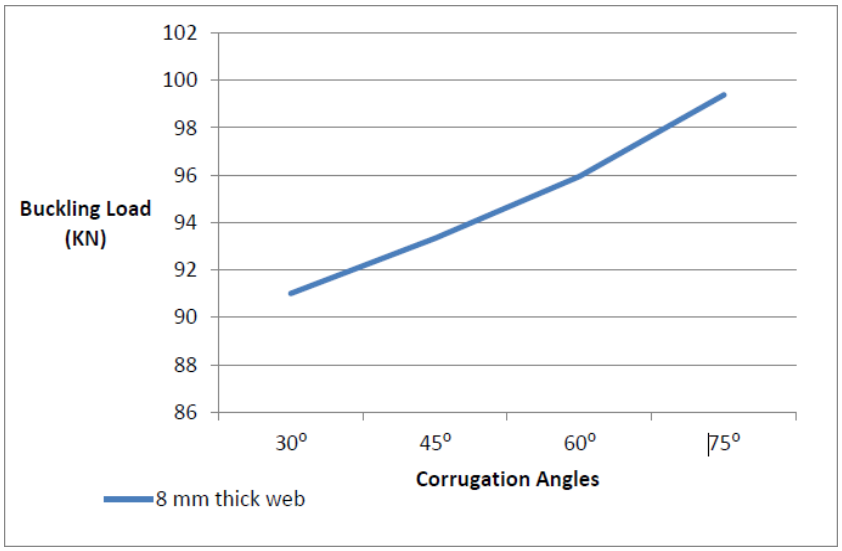

Fig. 10: Corrugation Angles' Impact on Buckling Load

Regarding a beam with consistent 150 mm length of the corrugation plate, wire width of 35 mm, and web thickness of 8 mm, The effect of corrugation angles on buckling load is shown in Figure 10. Figure 10 illustrates how the buckling stress rises in tandem with angles of corrugation. The upper limit buckling load is 75°. It is evident from Table 6 that both additional beams exhibit the similar pattern.

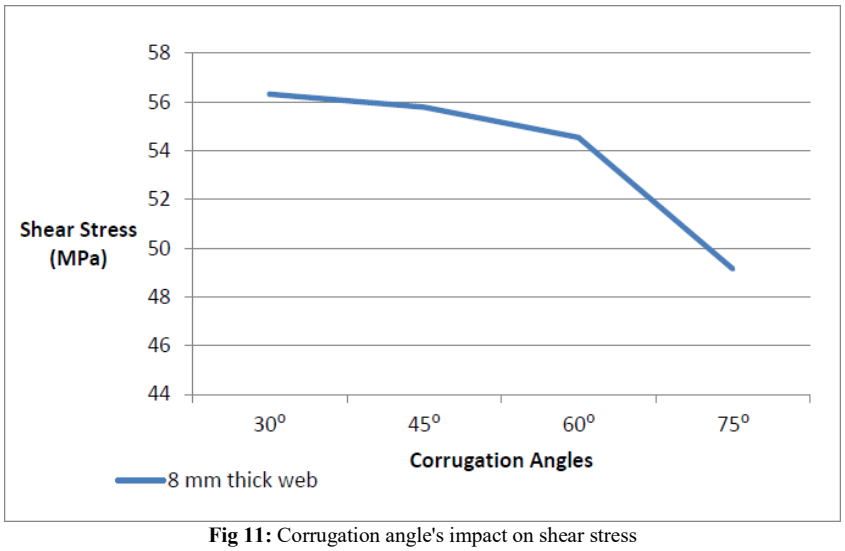

Fig 11: Corrugation angle's impact on shear stress

For a beam with an unaltered web size of 35 centimeters, an average web width of eight millimeters, and 150 mm curvature plates, Figure 11 illustrates the effect of a corrugation angle on shear stress. Figure 11 illustrates how the shear stress falls as the bending angle rises. The stress significantly decreases as the angle is raised from 60° to 75°.
The least quantity of stress occurs around 75°.Table 7 makes it clear that additional beams adhere to the same pattern.
For a structure having a constant net width of 35 mm, an outermost thickness of 8 mm, and a curvature plate that is 150 mm, Figure 12 illustrates how corrugation angles affect equivalent stress. Figure 12 shows that stress decreases with increasing corrugation angle, but this shift is minimal. At 75°, the least amount of stress happens. It is evident from Table 7 that the pattern is repeated by other beams.

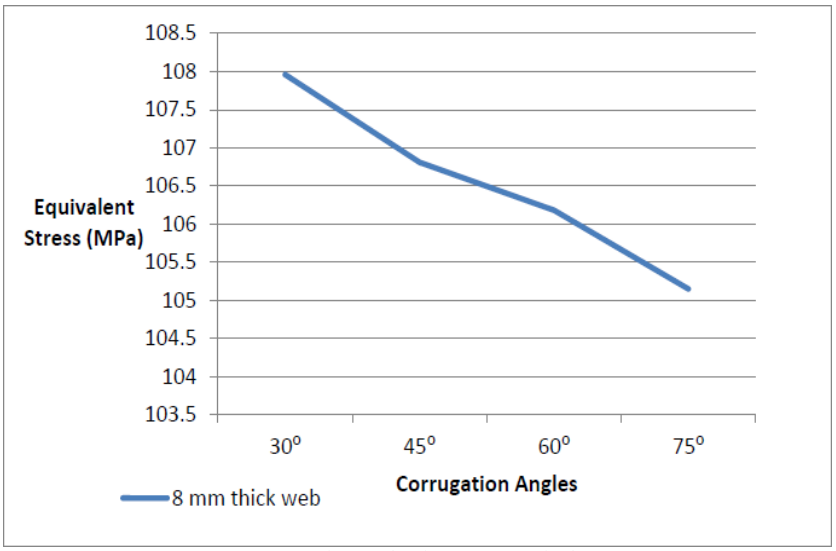

Fig 12: Corrugation angles' impact on equivalent stress

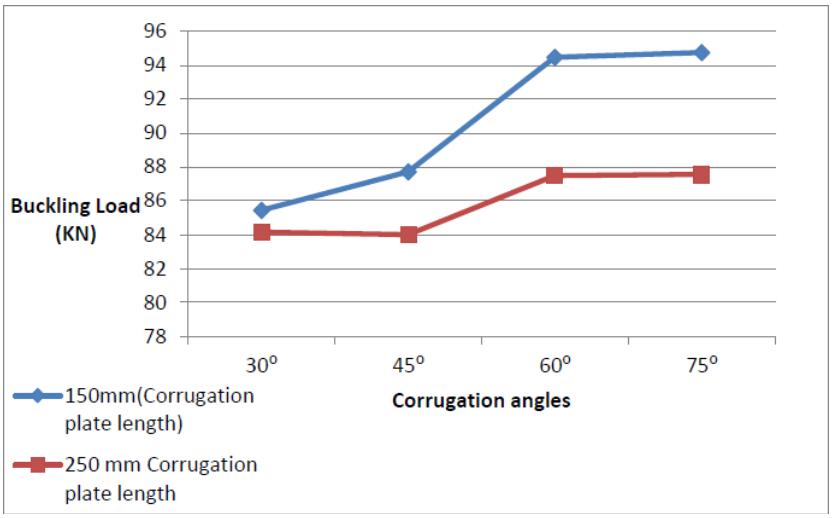

Fig 13. Corrugation plate length's impact on buckling load

Figure 13 illustrates how curvature plate length affects buckling load for a beam with varying curvature plate length of 150 and 250 mm, an even wire diameter of 35 mm, and a web width of 6 mm. As the curvature plate width increases from 150 to 250 mm, Figure 13 illustrates how the buckling stress decreases dramatically for each corrugation angle. At a corrugation angle of 75° and a plate measurement of 150 mm, the maximum buckling stress is achieved. It is evident from Table 6 that other beams exhibit the same pattern.

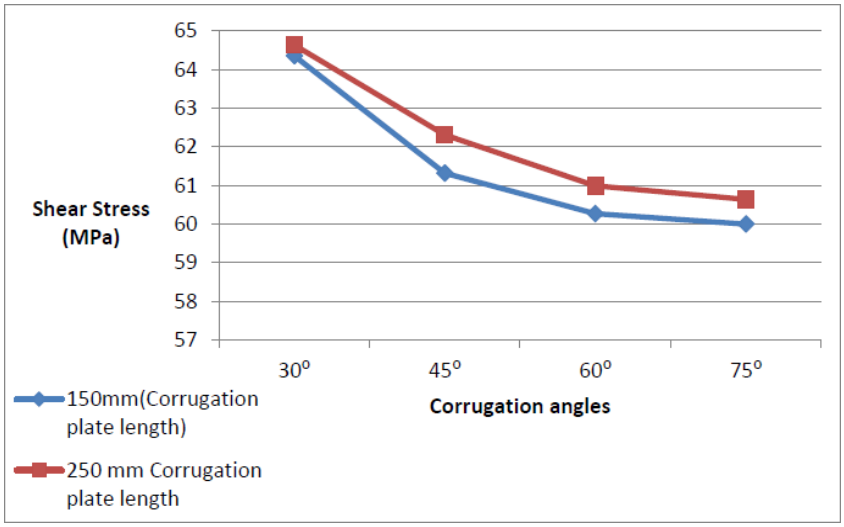

Fig 14: Corrugation plate length's impact on shear stress

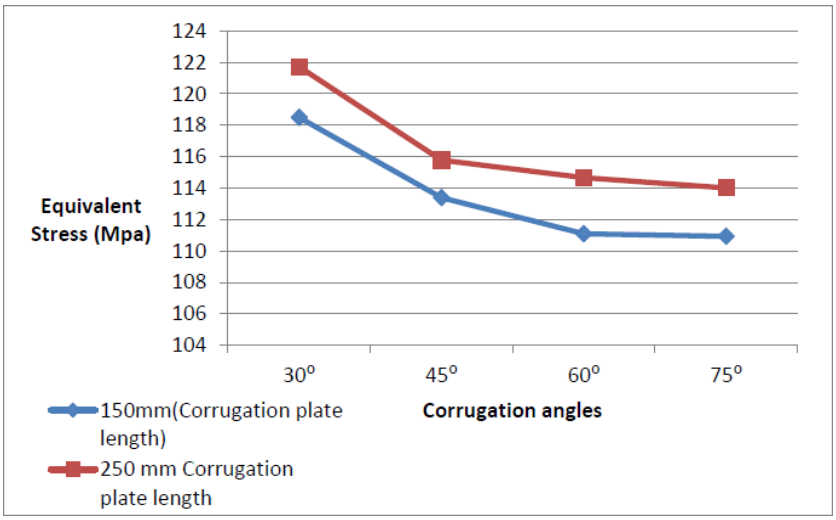

Fig 15: Length of Corrugation Plate and Equivalent Stress

For a beam with varying corrugation plate length of 150 having 250 mm, respectively, a constant net breadth of 25 mm, and a thickness of 6 mm, Figure 14 illustrates the effect of corrugation plate elevation on shear stress. Figure 14 shows that the stress caused by shear increases with plate length, with the least shear stress occurring at a 75° corrugation angle for a 150 mm plate length. It is evident from Table 7 that similar patterns are seen in other beams.

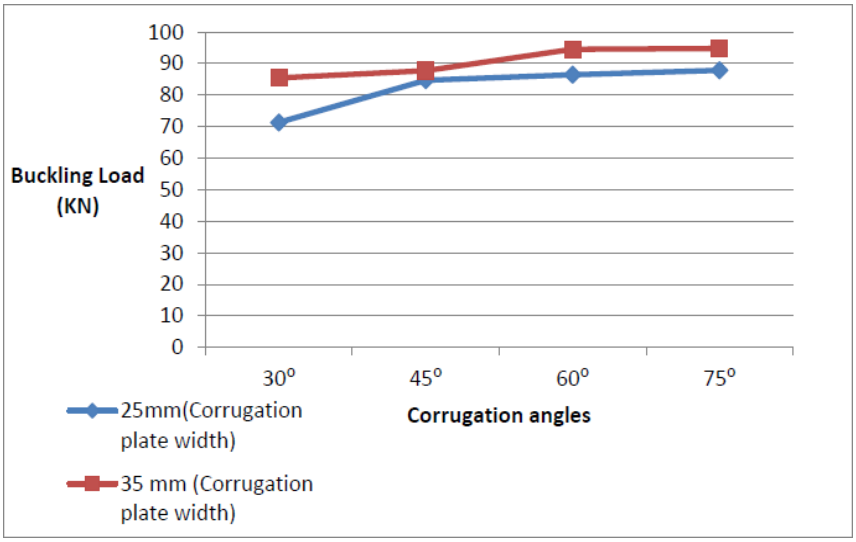

Fig 16. Corrugation plate width's impact on buckling load

With a constant web breadth of 25 mm and a thickness of 6 mm, Figure 15 illustrates how the total length of the curvature plates influences the corresponding stress for the beam with varied curvature plate lengths of 150 and 250 mm. It is evident from Figure 15 that as plate length grows, so does the associated stress. The least amount of tension is produced by a 150 mm plate width and a 75° corrugation angle. It is evident from Table 8 that more beams exhibit the same pattern.

The impact of the corrugation plate widths on bending load is depicted in Figure 16 for a beam with a constant curve plate length of 150 mm, a variable web width of between 25 and 35 mm, and a web layer depth of 6 mm. It is evident from Figure 16 that the buckling load increases with web width, reaching its maximum at 35 mm and a corrugation angle of 75°. It is evident from Table 6 that other beams follow the same trend.

For a system with a variable web broad of 25 to 35 mm, an exterior layer at a thickness of 6 mm, as well as an ongoing deformation plate length of 150 mm, Figure 17 illustrates how curvature plate width affects shear stress. As web width grows, shear stress reduces, as seen in Figure 17, with the lowest strain happening at a 75° curvature angle and a web width of 35 millimeters. Table 7 makes it clear that additional beams adhere to the same pattern

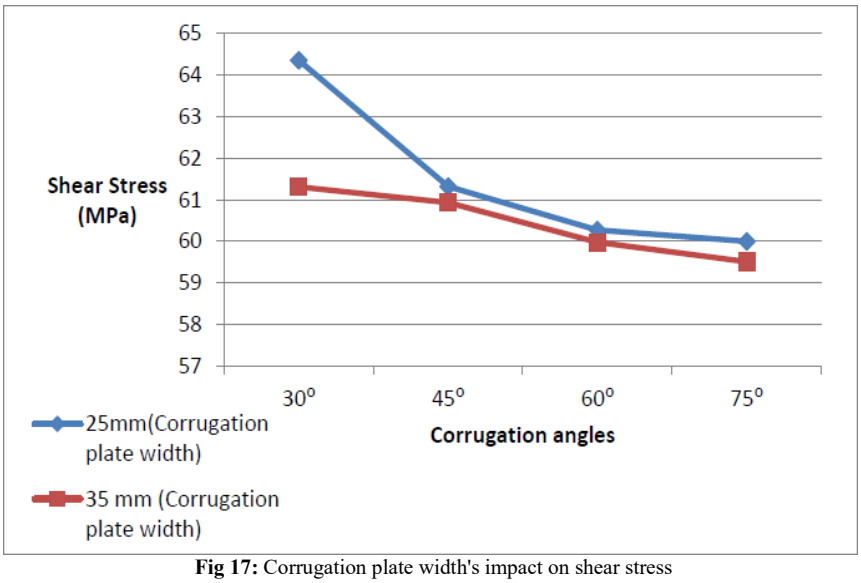

Fig 17: Corrugation plate width's impact on shear stress

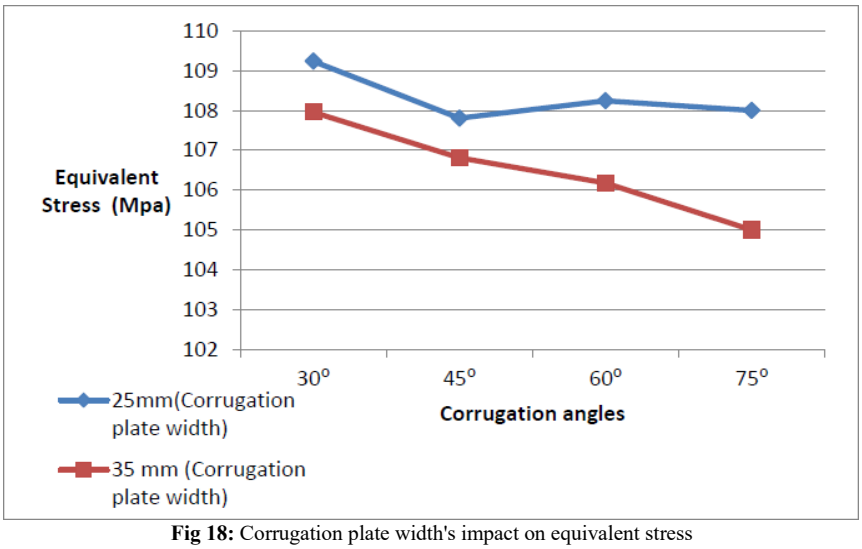

Fig 18: Corrugation plate width's impact on equivalent stress

Figure 18 illustrates how the corresponding stress for a structure with an adjustable webbing width of 25 to 35 mm is affected by the length of a curvature plate, a web size of 8 mm, and a constant curved plate measure of 150 m.
Shear equivalent decreases as web width increases, but this difference is minimal, as Figure 18 illustrates. The smallest amount of shear stress is produced by a web width of 35 mm and a corrugation angle of 75°. Table 8 makes it clear that additional beams adhere to the same pattern.

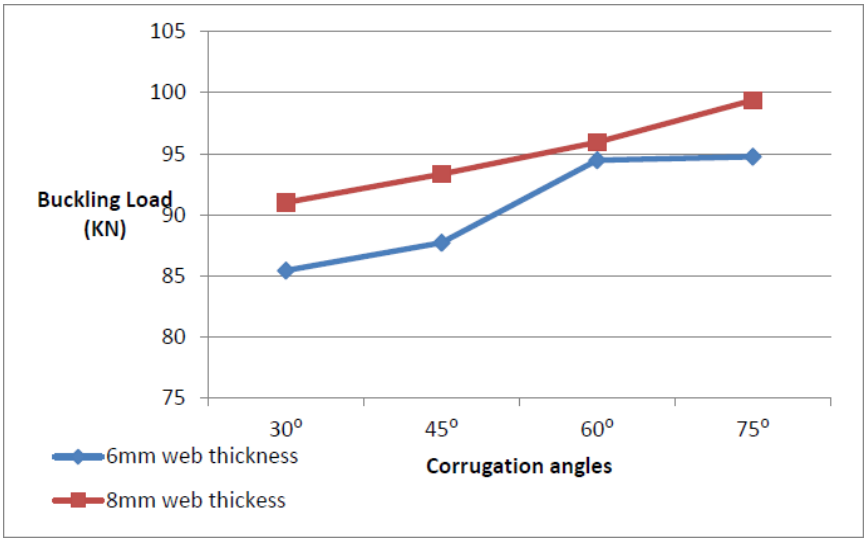

Fig 19: Corrugation plate thickness's impact on buckling load

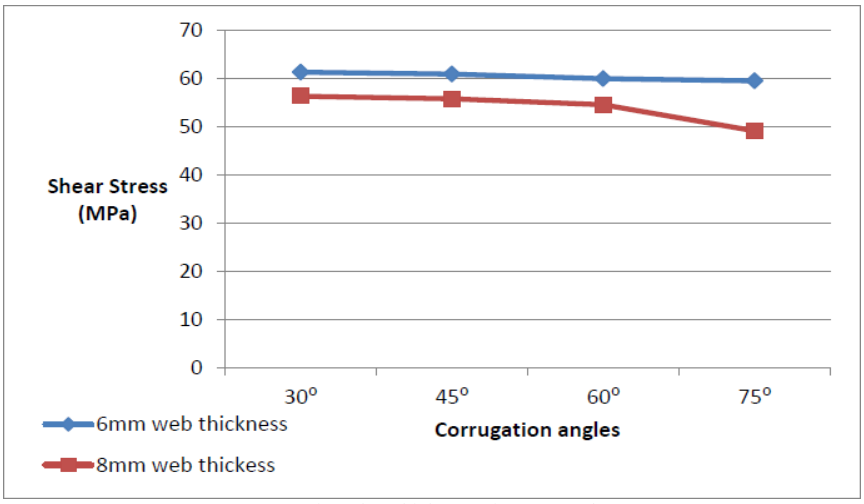

Fig 20: Corrugation plate thickness's impact on shear stress

Using a standard curvature plate measurement of 150 mm, an average web length of 35 mm, or varying web thicknesses of 6 and 8 mm, respectively, Figure 19 illustrates how corrugation plate thickness affects buckling stress. Figure 19 illustrates how the buckling load rises with web thickness. The greatest buckling force is achieved at a corrugation angle of 75° and a web thickness of 8 mm. It is evident from Table 6 that other beams follow the same trend. For a beam with a set curve plate span of 150 mm, an average online width of 35 mm, and varying web thicknesses of 6 and 8 mm, respectively, Figure 20 illustrates how corrugation plate thickness affects shear stress. Shear stress decreases with increasing web thickness, however this decrease is quite modest (Figure 20). A 75° corrugation angle and an 8 mm web thickness result in the lowest shear stress. Table 7 makes it clear that additional beams adhere to the same pattern.

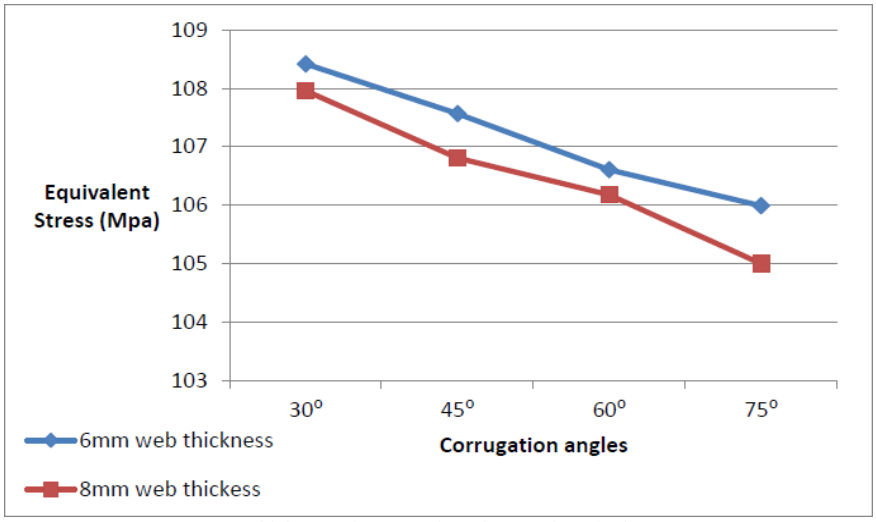

Fig. 21: Thickness of Corrugation Plates and Equivalent Stress

For a beam with a constant curved plate of 150 centimeters in length, a web width of 35 inches, and varying web thicknesses of six and eight mm as a respectively, Figure 21 illustrates how corrugation plate thickness affects equivalent stress. Figure 21 shows that although this shift is minimal, equivalent stress reduces as web thickness increases. At a 75° corrugation angle and 8 mm web thickness, the least amount of stress is experienced. It is evident from Table 7 that other beams follow the same pattern.

In order to improve resistance to laterally torsional buckling, the study offers a new approach to jib crane beam design that makes use of a trapezoidal perforated web. The effectiveness of the suggested corrugated netting beams and the traditional flat web beam was compared using finite element analysis (FEA). The findings show that by providing greater toughness against lateral torsion buckling and lowering shear, equivalent, and main loads, the hexagonal corrugated web beam considerably enhances structural performance.

With a corrugation inclination of 60°, a web width of 35 mm, 6 mm for the web width and 150 mm for the curvature plate, Model 13 showed the best performance, providing a higher buckling load yet being more lightweight and cost-effective than flat web beams. While longer corrugated plates decreased buckling resistance, other parameters like increased web width, thickness, and specific curving angles (75°) boosted it. These results demonstrate how trapezoidal columnar web designs can increase jib cranes' structural stability and efficiency.

7. Conclusion

The analysis of finite elements is a highly valuable method for carrying out optimization. Based on the facts presented above, it is possible to conclude that booms with support deform far less than booms without. The stress pattern demonstrates that the vertical column experiences the most stress when it comes into contact with the short column. This tension can be reduced by making design changes at the contact surface.

This work presents a novel design technique to create a jib crane beam using a trapezoidal web waves to investigate the beam's lateral torsional bending behaviour under Self weight plus a hoisted Load at the liberty end. After carrying out an analysis using finite elements for the jib crane's circular beams and compared it to the proposed corrugated web beams, these findings were reached:

1. Lateral torsion bending was less likely to occur in steel I beams having trapezoidally perforated webs. in contrast to typical I beams made of steel with flat webs.
2. A steel I beam that has a trapezoidal convex web experiences lower shear, comparable, or primary loads compared to a typical steel I have a flat web and I glow.
3. The Model 13, which is smaller and less expensive than the flat beam, provides stronger buckling stress due to its 150 mm curved sheet, 35 mm cable lengths, The web width is 6 mm, and the curvature angle is 60°.

8. Scope for Future Work

1. Experimental Validation: Future work may include developing experimental testing to validate the mathematical calculations performed in this study. Physical testing of crane prototypes and components confirms the correctness and dependability of numerical models, ensuring that theoretical predictions match real-world performance.
2. Composite Sections Analysis: Further research could include numerical evaluation of composite sections like hybrid materials and advanced composite I-beams. This would investigate the possible advantages of employing composite materials for jib crane design, which might enhance strength-to-weight ratios or overall performance.

Acknowledgment

I want to take this opportunity to thank and show our love for our project guide from Nagpur's Tulsiramji Gaikwad Patil College of Engineering and Technology, who provided us with the direction and space to accomplish this assignment.

References

[1] Dandavatimath, C. C., and H. D. Sarode. (2017). Finite element analysis and optimization of jib crane boom. *International Journal of Innovative Research in Science, Engineering and Technology* 6(7): 14287–14294.
[2] Denan, Fatima, C. K. Keong, and N. S. Hashim. (2017). The effects of the depth of web on the bending behaviour of triangular web profile steel beam section. *AIP Conference Proceedings* 1892: 020022, 1–8.
[3] Stefano, B., P. Bertolini, L. Taglialegne, and P. S. Valvo. (2016). Conference paper on shear stresses in tapered beams. *21st Italian Conference on Computational Mechanics*, Lucca, 83–84.
[4] Patil, T., and N. L. Shelke. (2016). Structural analysis of a cantilever beam with tapered web section through FEA. *Journal of Steel Structures and Construction* 2(2): 1–6.
[5] Dhanusha, M., and V. G. Reddy. (2016). Detail design and analysis of a free standing I beam jib crane. *International Research Journal of Engineering and Technology* 3(12): 193–203.
[6] Amreeta, R. K., and V. Singh. (2015). Design and stress analysis of single girder jib crane. *International Journal of Engineering Research and Technology* 4(9): 932–936.
[7] Rajmane, S. M., and A. Jadhav. (2015). Finite element analysis of jib crane. *International Journal of Innovative Research in Technology* 2(6): 404–407.
[8] Chaudhary, A. S., and S. N. Khan. (2015). Design and analysis of varying cross sectional cantilever beam with trapezoidal web for jib crane. *International Engineering Research Journal* Special Issue 2: 4475–4480.
[9] Kapadni, K. R., and S. G. Ganiger. (2015). Review paper on design and structural analysis of simply supported gantry crane beam for eccentric loading. *International Research Journal of Engineering and Technology* 2(8): 1622–1626.
[10] Kiranalli, S. S., and N. U. Patil. (2015). Jib crane analysis using FEM. *International Journal for Scientific Research and Development* 3(4): 185–189.
[11] Wan, H. X., and M. Mahendran. (2015). Bending and torsion of hollow flange channel beams. *Engineering Structures* 84: 300–312.
[12] Bollimpelli, K. S., and V. R. Kumar. (2015). Design and analysis of column mounted jib crane. *International Journal of Research in Aeronautical and Mechanical Engineering* 3(1): 32–52.
[13] Kumar, V. C. Arvind. (2015). Design and analysis of beam for deformation of floor mounted jib crane. M.Tech Thesis, Gujarat Technical University.
[14] Khetre, N. S., P. S. Bankar, and A. M. Meshram. (2014). Design and static analysis of I section boom for rotary jib crane. *International Journal of Engineering Research and Technology* 3(8): 1071–1074.
[15] Divahar, R., and P. S. Joanna. (2014). Lateral buckling of cold formed steel beam with trapezoidal corrugated web. *International Journal of Civil Engineering and Technology* 5(3): 217–225.
[16] Ozbasaran, H. (2014). A parametric study on lateral torsional buckling of European IPN and IPE cantilevers. *International Journal of Civil, Architectural, Structural and Construction Engineering* 8(7): 783–788.
[17] Trahair, N. (2014). Bending and buckling of tapered steel beam structures. *Engineering Structures* 59: 229–237.
[18] De'nan, Fatimah, M. Mustar, A. B. Hassan, and N. Omar. (2013). Effect of triangular web profile on the shear behaviour of steel I-beam. *Iranica Journal of Energy & Environment* 4(3): 219–222.
[19] Suratkar, A., V. Shukla, and K. S. Zakiuddin. (2013). Design optimization of overhead EOT crane box girder using finite element analysis. *International Journal of Engineering Research & Technology* 2(7): 720–724.
[20] Limaye, A. A., and P. M. Alandkar. (2013). Strength of welded plate girder with corrugated web plate. *International Journal of Engineering Research and Applications* 3(5): 1925–1930.
[21] Gerdemeli, I., S. Kurt, and B. Tasdemir. (2012). Design and analysis with finite element method of jib crane. *Mechanical Engineering, Istanbul Technical University – Turkey*, 565–568.
[22] Wakchaure, M. R., and A. V. Sagade. (2012). Finite element analysis of castellated steel beam. *International Journal of Engineering and Innovative Technology* 2(1): 365–372.
[23] De'nan, Fatimah, and N. S. Hashim. (2011). The effect of web corrugation angle on bending performance of triangular web profile steel beam section. *International Journal of Environmental Protection* 1(5): 53–56.
[24] De'nan, Fatimah, M. H. Osman, and S. Saad. (2010). The study of lateral torsional buckling behaviour of beam with trapezoid web steel section by experimental and finite element analysis. *International Journal of Recent Research and Applied Studies* 2(3): 232–240.
[25] Gerdemeli, I., S. Kurt, and H. O. Alkan. (2010). Main girder beam design and finite element analysis of 2x160 ton gantry crane. *14th International Research/Expert Conference on Trends in the Development of Machinery and Associated Technology*, Mediterranean Cruise, 565–568.
[26] Moon, J., J. W. Yi, B. H. Choi, and H. E. Lee. (2009). Lateral torsional buckling of I girder with corrugated webs under uniform bending. *Thin-Walled Structures* 47(1): 21–30.
[27] Brettle, M. (2005). Lateral torsional buckling and slenderness. *Technical Paper, New Steel Construction*, 30–34.
[28] Sapalas, V., M. Samofalov, and V. Saraskinas. (2005). Finite element stability analysis of tapered beam-columns. *Journal of Civil Engineering and Management* 11(3): 211–216.
[29] Lee, J., S. E. Kim, and K. Hong. (2002). Lateral buckling of I section composite beams. *Engineering Structures* 24: 955–964.

[30] Gupta, P., S. T. Wang, and G. E. Blandford. (1995). Lateral torsional buckling of non-prismatic I beams. *Journal of Structural Engineering* 122(7): 748–755.
[31] Raut, J. M., P. B. Pande, B. V. Bahoria, R. M. Bhagat, M. A. Kumbhalkar, T. S. Sargar, and M. Sakhlecha. (2025). Dynamic analysis and balancing of railway tracks supported by concrete sleepers. *African Journal of Applied Research* 11(1), January. https://doi.org/10.26437/ajar.v11i1.885
[32] Sahare, Pramod H., Narendra K. Ade, Manoj A. Kumbhalkar, Kishor S. Rambhad, Shivani D. Polshettiwar, Sourav A. Paul, Tejas N. Vaidya, and Rushikesh S. Janwe. (2023). Manufacturing of foldable bicycle with finite element analysis of push-pull clamp. *AIP Conference Proceedings* 2839. https://doi.org/10.1063/5.0167693